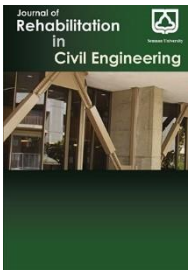

journal homepage: http://civiljournal.semnan.ac.ir/

# Experimental Study on RC Deep Beams with Non-Prestressed Tendons as Main Reinforcement

**Seyed Mohammad Reza Mortazavi[1*], Milad Shakiba[1]**

1. Department of Civil Engineering, Shahid Rajaee Teacher Training University, Tehran, Iran.
Corresponding authors: mortazavi@sru.ac.ir

**ARTICLE INFO**

Article history:
Received: 07 May 2021
Revised: 13 February 2022
Accepted: 14 February 2022

Keywords:
Beam;
Rebar;
Tendon;
Non-prestressed;
Reinforced concrete.

**ABSTRACT**

In the present study, The main purpose is to focus on the applicability of using non-prestressed tendons as the main reinforcement in concrete beams. Therefore, the main reason for the analytical study is to develop a model that can predict the flexural behavior of RC beams with ordinary reinforcements and/or with non-prestressed tendons (cables). An experimental program, as well as a computational program, was designed to see the behavior of such concrete reinforced beams. To do so, 9 beam models of one concrete mix were cast. The beams were cast in accordance with ACI recommendations and all tests were conducted under the same condition. The beams tested include two types of beams with ordinary steel rebar and with cables (tendons). The beams studied in this research are classified as deep beams (L/h<4); so the effect of shear deformations was considered. In addition, test results were compared with the predicted theoretical values. The theoretical model was able to predict the experimental load-deflection curves almost accurately. Therefore, it was demonstrated that the same concepts of the normal reinforced concrete beams can be applied for reinforced concrete beams using tendons as main reinforcement for both stiffness and strength calculations. Also, the same methodology used in concrete beams with steel rebar is applicable to the ones with non-prestressed tendons. The results showed that using the nominal flexural strength equations of regular reinforced concrete beams can accurately predict the strength of the beams with cables.

## 1. Introduction

The concrete enclosed steel members, known as "steel Reinforced Concrete (SRC)", are widely used in building structures. Extensive experiments have been performed on SRC specimens to investigate static behavior and

**How to cite this article:**
Mortazavi, S., Shakiba, M. (2023). Experimental Study on RC Deep Beams with Non-Prestressed Tendons as Main Reinforcement. Journal of Rehabilitation in Civil Engineering, 11(1), 43-59.
https://doi.org/10.22075/JRCE.2022.23355.1509

seismic performance [1–8]. These studies have shown that the SRC structure has high stiffness, high load carrying capacity, ductility, and energy dissipation capacity [9-11]. This paper is to show that if tendons are used as the main reinforcement, in regular RC beams (non-prestressed), the stiffness and strength of the beam can be predicted with similar concepts used in RC beams using rebar. So, when the stiffness and strength characteristics of these beams, determined by the principles of mechanics, are shown to be in good agreement with the test results, it means that the tendons are doing what they were expected to do. For example, the same ductility concepts of RC beams are shown to be still valid when different ratios of tendons are used; under-reinforced, balanced, and over-reinforced [12].

Tao et al. [13] worked on experimental research to investigate the effects of the presence of non-prestressed reinforcement and its influence on the fps value. In total, they tested 22 partially prestressed beams, with unbonded tendons and under third point loading. The variables were the area of prestressed and ordinary steel and compressive concrete strength. Campbell and Chouinard [14] loaded six partially prestressed concrete beams with unbonded tendons with third-point loads to study the effect of non-prestressed bonded reinforcement on unbonded prestressing steel at ultimate state. The only parameter considered was the amount of non-prestressed tensile steel. They discovered that while the amount of prestressing steel remains the same, adding high amounts of mild steel results in a decrement in unbounded prestressing steel at the ultimate state.

An et al. [15] provided a model to investigate the stress and force of reinforced concrete beams with externally applied fibre composite plates (GFRP). Using classical bending theory and strain compatibility, the effects of variables such as material strength, modulus of elasticity, and reinforcement ratios of the steel and GFRP were compared with experimental results of the previous experiment [16]. The behavior of the beams was well predicted using the model [17-20], [41]. Triantifillou et al. [21] used strain compatibility and fracture mechanics to analyze reinforced concrete beams applied with externally bonded Carbon Fiber Reinforced Polymers (CFRP). The same assumptions of An et al. [15] were used by including the rectangular compressive stress distribution in concrete during failure. The applied moment that cause each of the three failure modes were predicted. The failures were yielding of the Steel Reinforcement (SR) followed by CFRP rupture; yielding of the steel reinforcement followed by the crushing compression zone of concrete, and crushing of concrete before failure of any tensile components. The proposed models were compared with experimental studies and were considered valid [22-26]. Bhutta [27] provided the moment, stiffness, and deflection model of reinforced concrete beams with applied fibre-reinforced polymer (FRP). Glass, carbon, and kevlar fiber reinforced plastics were utilized. Beams reinforced with kevlar showed the highest increase in moment capacity and stiffness, while the smallest were the beams reinforced with glass. The moment capacity of beams reinforced with carbon fell between these two composites [28,29].

Alkhairi and Naaman [30] proposed a nonlinear numerical model for predicting the moment versus deflection response of partially prestressed concrete beams, whether simply supported or continuous, with internal or external unbonded tendons. This model utilizes an iterative procedure for calculating stress in

the unbonded tendon by the means of a nonlinear analysis at various sections of the member [31-34]. With the increase in failure of high-strength steel tendons in prestressed concrete structures, Yuyama et al. [35] conducted basic studies using acoustic emission techniques. Three types of post-tensioned concrete beams with a steel bar, strand, and parallel wire cable were tested in a laboratory. It was proven that the technique used is a very useful technique to detect and evaluate failures of high-strength steel tendons in prestressed concrete bridges.

Although some researchers have focused on the flexural behavior of reinforced concrete beams with ordinary reinforcements, while In the present analytical study, an experimental program, as well as a computational program, have been considered to create a model that can predict the flexural behavior of reinforced concrete beams with ordinary reinforcements and/or with non-prestressed tendons (cables). In this regard, 27 beam specimens (nine models) were cast by ACI and ASTM recommendations and tested under the same condition.

## 2. Experimental procedure

### 2.1. Specimen Description

In the present study, twenty-seven $180 \times 200 \times 600\ mm$ beam specimens (nine models) have been cast and cured until 28 days in accordance with ACI 318, ACI 308R and ASTM C150 recommendations [36-38]. Before pouring concrete, the steel cages including longitudinal steel (rebar or tendon), and transverse reinforcements (made with rebar only), were assembled and put in the molds with the specified clear cover from each side. Then they were tied to the molds to prevent movement due to the dynamic effects of concrete placement. The molds were filled with concrete and each one of the specimens was tested on the corresponding $28^{th}$ day. To observe the performance of cables (tendons) in different ductility levels, the beams were with three levels of longitudinal reinforcements to represent under reinforced, balanced, and over reinforced beam sections. This was to know if the same concept of regular reinforced concrete beams applies for beams with non-prestressed cables (tendons) as the main reinforcement.

### 2.2. Material Properties

#### 2.2.1. Concrete

In the present study, one normal concrete (NC) mix design is used. The specimens were prepared using Type II Portland cement, whose specific surface was 3050 $cm^2/gr$, and its chemical specifications are presented in Table 1. Natural river sand with fineness modulus of about 3.0 and natural river gravel with a maximum nominal size of 19 mm have been used as fine and coarse aggregate, respectively. Three standard cylinder specimens with dimensions of 150 × 300 mm were tested after 28 days and the average compressive strength of concrete was 39.6 MPa. The concrete mix design and properties are provided in Table 2 [39].

#### 2.2.2. Steel bars and tendons

For this experiment, steel bars with diameters of 10, 12, and 22 mm and steel tendons with diameters of 6 and 10 mm, were used. A preliminarily tensile test was conducted to ensure the tendons would not deform or rupture during subsequent loading. Table 3 shows the mechanical properties of the steel bars (A3-S400) and tendons (GR.270).

**Table 1.** Chemical properties of the cement.

| Material | Chemical analysis (%) | | | | | | | | |
|---|---|---|---|---|---|---|---|---|---|
| | $SiO_2$ | $Al_2O_3$ | $Fe_2O_3$ | CaO | MgO | $SO_3$ | $Na_2O$ | $K_2O$ | L.O.I |
| Cement | 21.8 | 4.85 | 3.53 | 63.43 | 1.52 | 2.13 | 0.36 | 0.56 | 1.83 |

**Table 2.** Composition and characteristics of concrete.

| Concrete type | W/C | Water ($kg/m^3$) | Cement ($kg/m^3$) | Sand 0–4 mm ($kg/m^3$) | Gravel 4–20 mm ($kg/m^3$) | Average compressive strength (MPa) | Slump (mm) |
|---|---|---|---|---|---|---|---|
| NC | 0.41 | 184.5 | 450 | 762 | 1139 | 39.6 | 65 |

**Table 3.** Material properties for steel reinforcements.

| Steel bar | | | Steel tendon | |
|---|---|---|---|---|
| Yield strength (MPa) | Ultimate strength (MPa) | Elastic modulus (GPa) | Ultimate strength (MPa) | Elastic modulus (GPa) |
| 400 | 600 | 200 | 1860 | 192-208 |

## 2.3. Set up and Instrumentation

All beams were tested to failure under four points or three points loading. The tests were performed using a universal mechanical testing machine. The beam deflection at mid-span was measured using a linear variable differential transformer (LVDT) with a precision of 0.025 mm and a data logger. The loading rate was about 1 mm/min and all tests were carried out under the same condition and the load applied and displacement of beams were recorded. The load was applied using stroke control at a low rate to prevent any rate dependency of loading in the results and it was continued until the beam failed. In some of these beams, the ultimate strength was governed by their end failure, above the support point with a local concrete crushing. To overcome this problem, some of these beams were tested by mid-span loading (three points loading) or changing the center to center of supports. Table 4 presents detailed information on the experimental program. Fig. 1 shows the used test setup configuration (The unit of measurement is mm).

**Table 4.** Specimens' characteristics details on the experimental program.

| ID | Steel Type | Main Steel | Stirrups | C/C of Supports (mm) | Type of bending test |
|---|---|---|---|---|---|
| RB-1 | Rebar | 3ϕ12mm | ϕ10mm@75mm | 450 | Four-point |
| RB-2 | Rebar | 3ϕ22mm | 2ϕ10mm@50mm | 450 | Four-point |
| RB-3 | Rebar | 3ϕ22mm | 2ϕ10mm@50mm | 500 | Four-point |
| RB-4 | Rebar | 4ϕ22mm | 2ϕ10mm@50mm | 450 | Four-point |
| CB-1 | Tendon | 3ϕ6mm | ϕ10mm@50mm | 500 | Four-point |
| CB-2 | Tendon | 3ϕ10mm | 2ϕ10mm@50mm | 500 | Four-point |
| CB-3 | Tendon | 3ϕ10mm | 2ϕ10mm@50mm | 500 | Three-point |
| CB-4 | Tendon | 4ϕ10mm | 2ϕ10mm@50mm | 450 | Four-point |
| CB-5 | Tendon | 4ϕ10mm | 2ϕ10mm@50mm | 400 | Four-point |

a)

b)

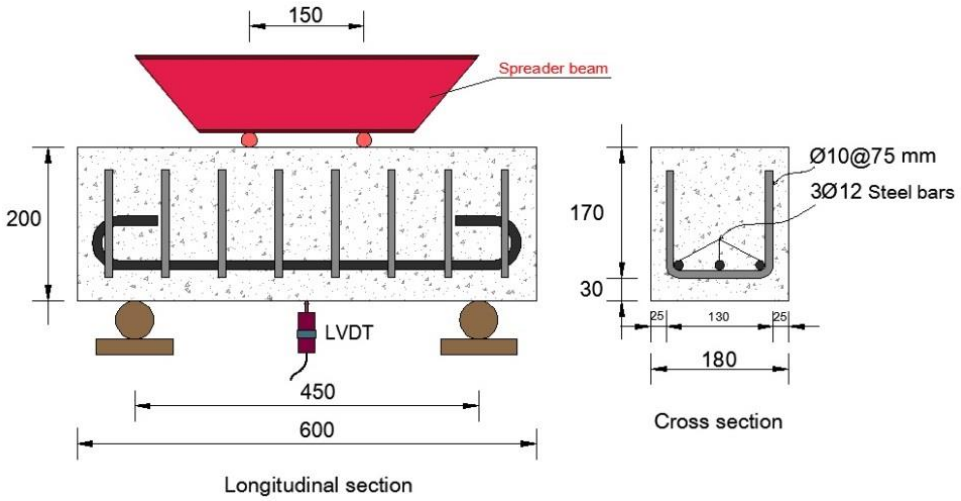
150
Spreader beam
200
LVDT
450
600
Longitudinal section
170
30
Ø10@75 mm
3Ø12 Steel bars
25
130
25
180
Cross section

c)

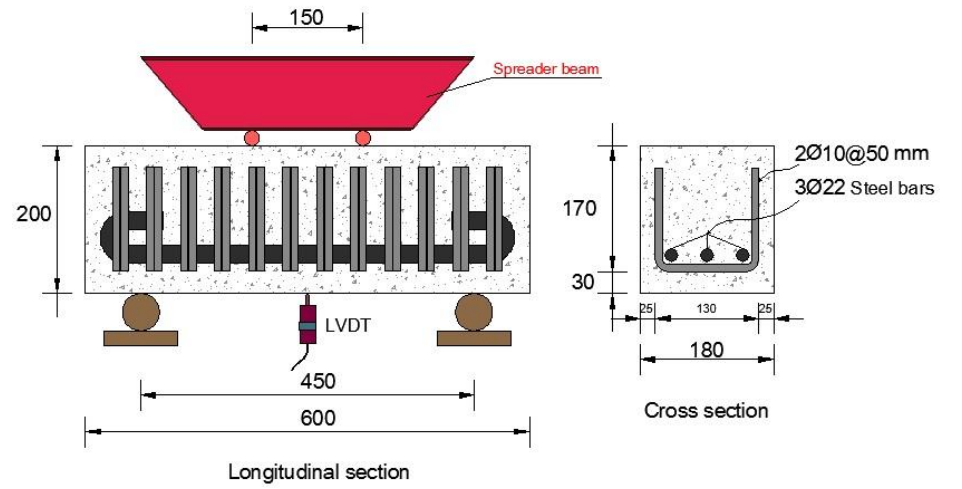
150
Spreader beam
200
LVDT
450
600
Longitudinal section
170
30
2Ø10@50 mm
3Ø22 Steel bars
25
130
25
180
Cross section

d)

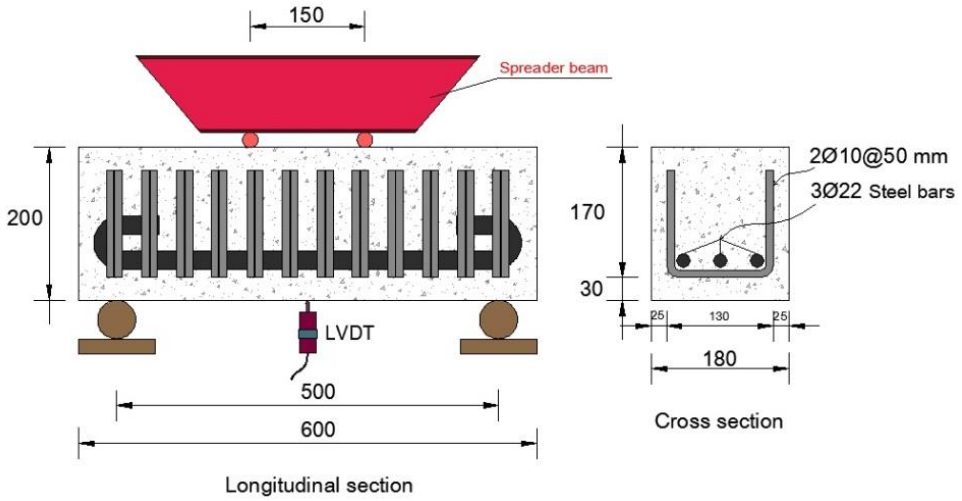
150
Spreader beam
200
LVDT
500
600
Longitudinal section
170
30
2Ø10@50 mm
3Ø22 Steel bars
25
130
25
180
Cross section

e)

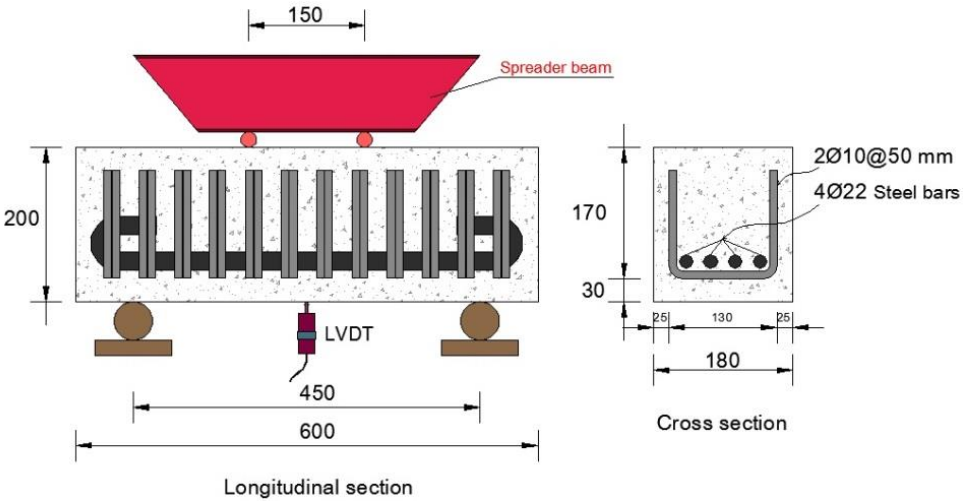
150
Spreader beam
200
LVDT
450
600
Longitudinal section
170
30
2Ø10@50 mm
4Ø22 Steel bars
25
130
25
180
Cross section

f)

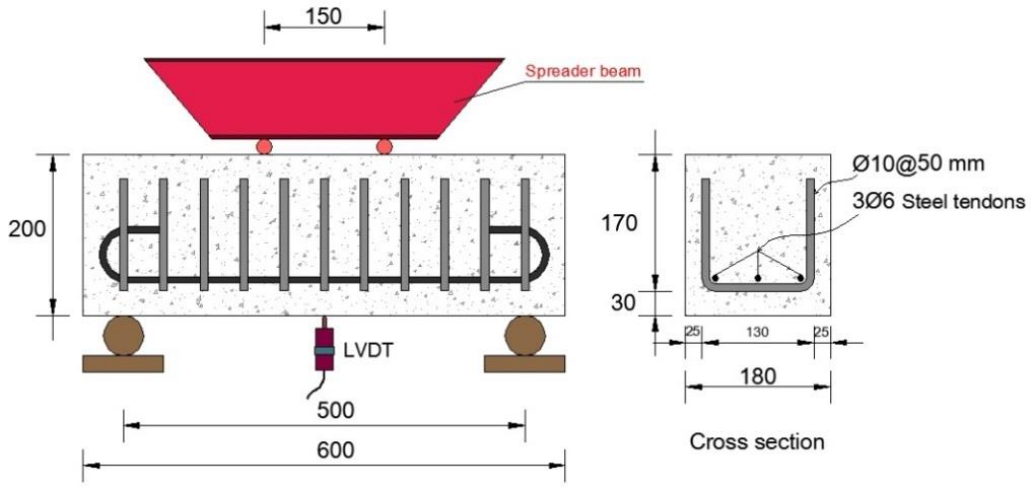
150
Spreader beam
200
LVDT
500
600
170
30
Ø10@50 mm
3Ø6 Steel tendons
25
130
25
180
Cross section

g)

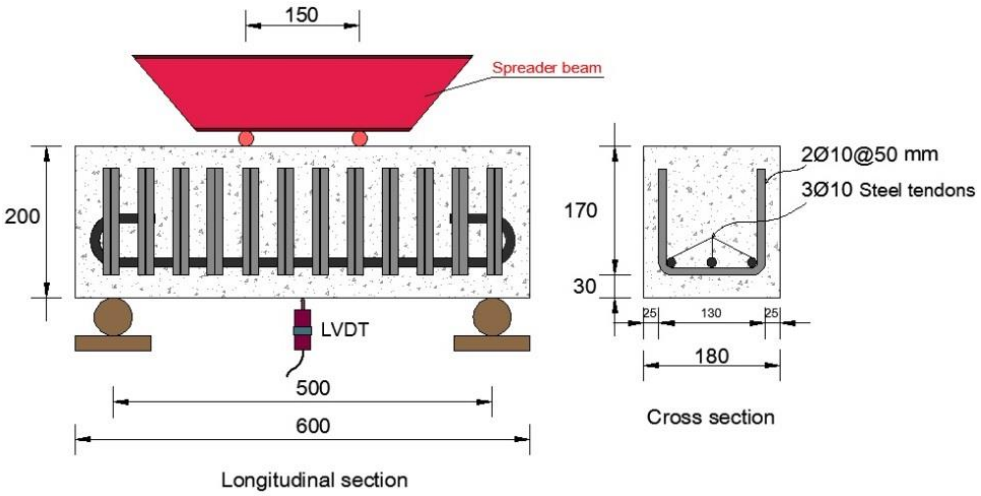
150
Spreader beam
200
LVDT
500
600
Longitudinal section
170
30
2Ø10@50 mm
3Ø10 Steel tendons
25
130
25
180
Cross section

h)

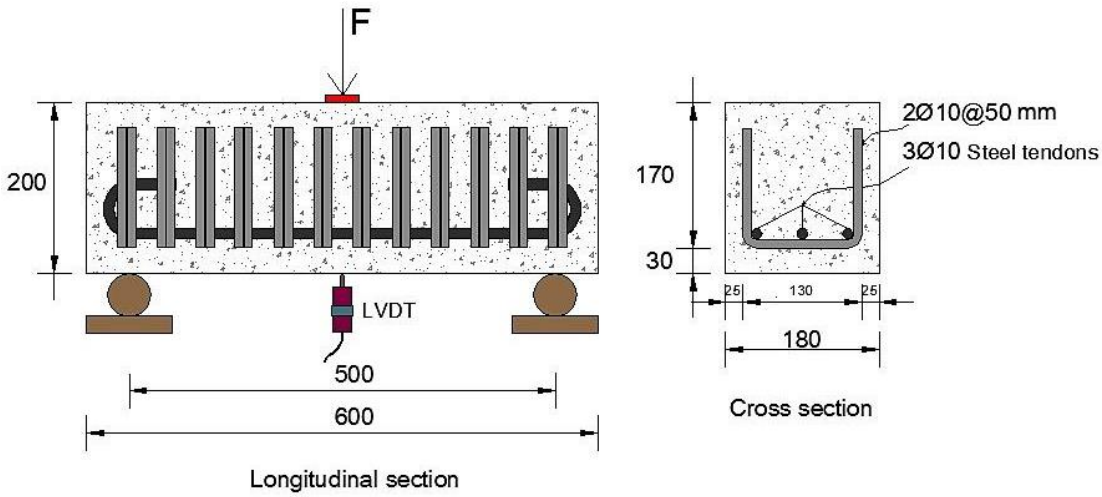
F
200
LVDT
500
600
Longitudinal section
170
30
2Ø10@50 mm
3Ø10 Steel tendons
25
130
25
180
Cross section

i)

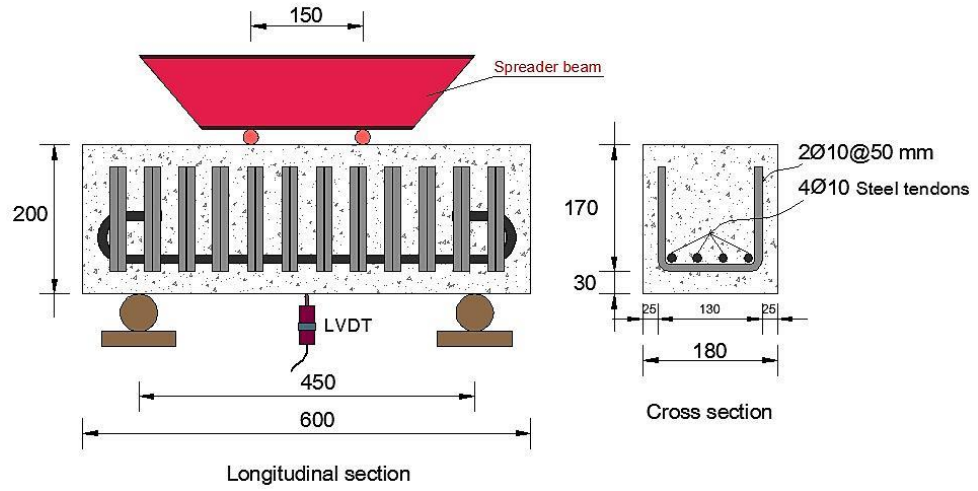


j)

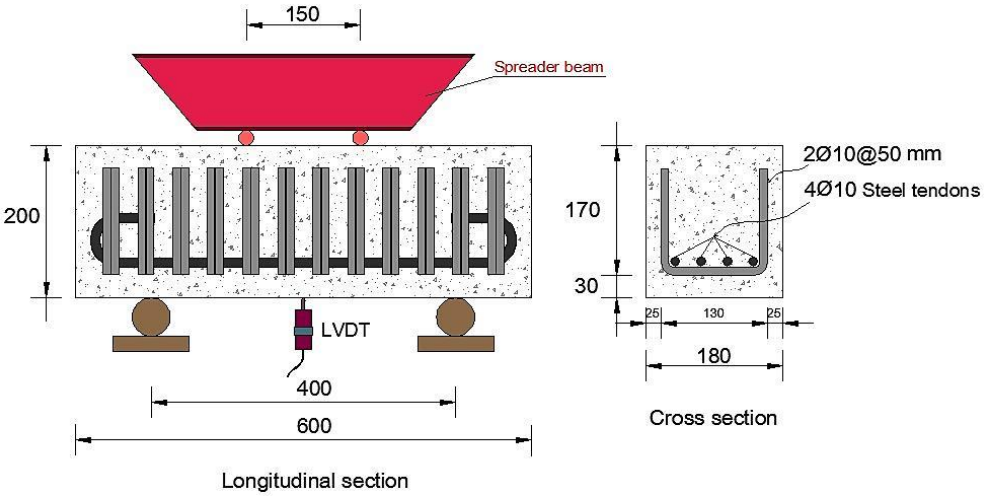


k)

**Fig. 1.** Setup configuration, a) Configuration of three-point bending test, b) Configuration of four-point bending test, c) RB-1 specimen, d) RB-2 specimen, e) RB-3 specimen, f) RB-4 specimen, g) CB-1 specimen, h) CB-2 specimen, i) CB-3 specimen, j) CB-4 specimen, and k) CB-5 specimen.

## 3. Analytical model

In this study, we intend to provide a model that can develop the flexural behavior of RC beams with ordinary reinforcement or with non-prestressed tendons. The model was also used to forecast the nominal capacity. To predict the load-deflection curve and ultimate capacity of the beams, calculations are carried out in two stages; moment-curvature and then load-deflection calculations. For the first part, we needed to have the constitutive properties of concrete as well as cables and rebar. Stress-strain models for concrete and rebar are illustrated in Figs. 2 and 3.

For concrete models $\varepsilon_0$= 0.002 was used and tensile strength was neglected. Concrete tensile strength is ignored and small flexural deformations are implemented and shear deformations were also considered in stiffness calculations. The stress-strain curve for concrete is approximated using Park and Paulay [40]; as shown in Fig. 2.

The stress-strain curve for the reinforcing steel is approximated; as illustrated in Fig. 3. The stress-strain curve for concrete is approximated by using two functions as shown in Fig. 2. The first equation is a parabolic function and is used up to the maximum compressive stress (f $'_C$). The other equation is linear and decreases from the maximum compressive stress to the maximum strain. For this model, a maximum concrete strain of 0.003 was used (which is conservative due to the confinement of the concrete caused by the stirrups). For cables (tendons), a bilinear approximation of the coupon test results was used; as shown in Fig. 4.

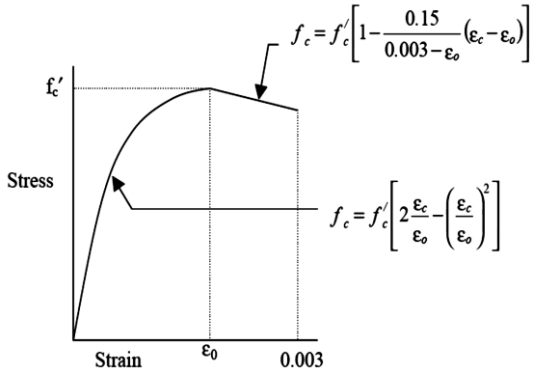


**Fig. 2.** Idealized stress-strain diagram of concrete material.

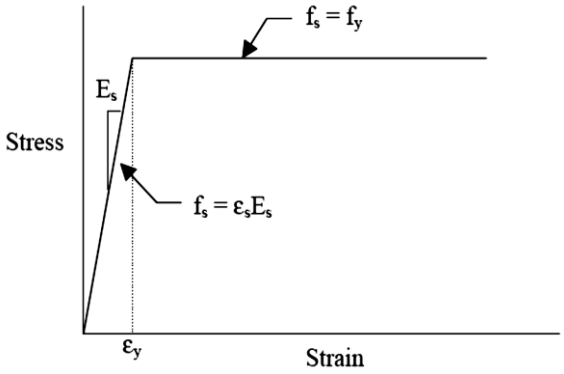


**Fig. 3.** Idealized stress-strain diagram of steel reinforcement material.

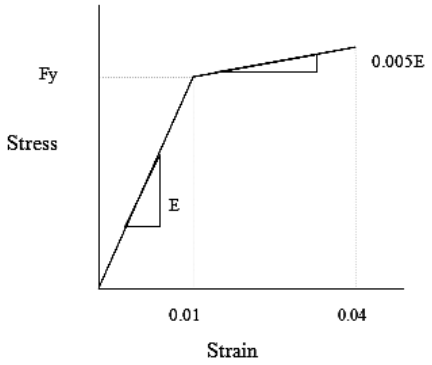


**Fig. 4.** Idealized stress-strain diagram of steel tendons (cables).

## 3.1. Moment-curvature

The first step to calculate the moment-curvature values is to locate the location of neutral axis for each value of curvature; as illustrated in Fig. 5.

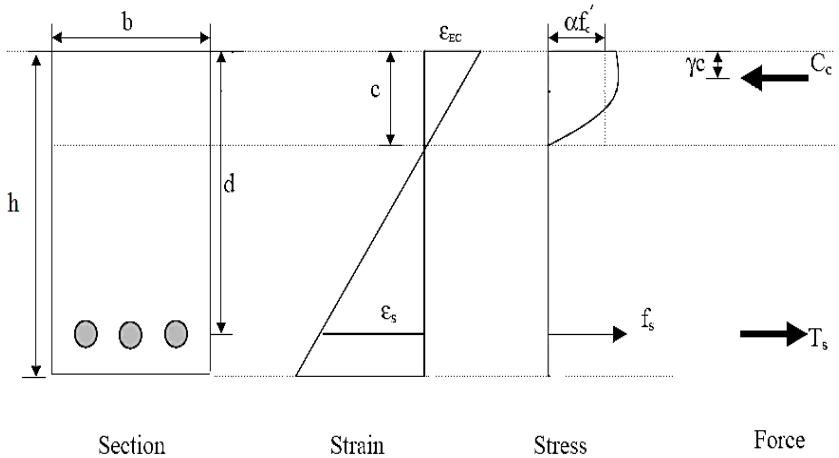


**Fig. 5.** Cross-section, strain distribution, stress distribution and resultant forces.

Using the equation of equilibrium as well as compatibility equations, tensile as well as compressive forces are obtained; as follows:

$$C_c = T_s \tag{1}$$

$$C_c = \int_0^c f_c \, dA = \int_0^c f_c \, b \, dy \tag{2}$$

$$T_s = A_s \, f_s \tag{3}$$

Where stress in concrete is;

$$f_c = \begin{cases} f_c' \left[ \dfrac{2\varepsilon_c}{\varepsilon_0} - \left( \dfrac{\varepsilon_c}{\varepsilon_0} \right)^2 \right] & if \quad \varepsilon_c \le \varepsilon_0 \\ f_c' \left[ 1 - \dfrac{0.15}{0.003 - \varepsilon_0} \left( \varepsilon_c - \varepsilon_0 \right) \right] & if \quad \varepsilon_c \ge \varepsilon_0 \end{cases} \tag{4}$$

And stress for cables is calculated as:

$$f_s = \begin{cases} E_s \, \varepsilon_s & if \quad \varepsilon_s \le \varepsilon_y \\ f_y + E_t \left( \varepsilon_s - \varepsilon_y \right) & if \quad \varepsilon_s \ge \varepsilon_y \end{cases} \tag{5}$$

And stress for rebar is calculated as:

$$f_s = \begin{cases} E \, \varepsilon_s & if \quad \varepsilon_s \le \varepsilon_y \\ f_y & if \quad \varepsilon_s \ge \varepsilon_y \end{cases} \tag{6}$$

And strain values for steel and compressive concrete area are as follows;

$$\varepsilon_s = \gamma \left( d - c \right) \tag{7}$$

$$\varepsilon_c = \gamma \, y \tag{8}$$

For every value of curvature, combining Equations 1-8, neutral axis (c) will be located. The next step is to calculate the strains in steel and concrete to check their failure status. Failure would occur if the extreme strain in concrete or cables reaches the ultimate values. These ultimate strain values are 0.003 for concrete and 0.04 for cables (Fig.s 2 and 4). If for the value of curvature, failure has not occurred, the next step is to calculate stresses using Equations 4-8. Now, the corresponding internal moment is determined as follows to complete the moment-curvature calculations.

$$M = f_s \, A_s \left( d - c \right) + \int_0^c y \, f_c \, b \, dy \tag{9}$$

## 3.2. Load-deflection

The beams studied in this research are classified as deep beams (L / h < 4); so the effect of shear deformation should be included. Therefore, to predict the load-deflection of the beams, two sets of calculations are performed; which are deflection due to bending moment, and deflection due to shear force and finally the results are added.

### 3.2.1. Deflection due to bending moment

To predict the bending deflection of the beam due to a specific value of applied load, first, the moment at any section is calculated and using the Moment-Curvature values calculated in the previous part, the curvature value at each section is determined. Now, using integration both the beam slope (θ) and deflection ($\delta_b$) are calculated; as follows:

$$\theta(x) = \int_0^x \gamma \left( M(\eta) \right) d\eta + \theta_0 \tag{10}$$

$$\delta_b(x) = \int_0^x \theta(\eta) \, d\eta + \delta_{b0} \tag{11}$$

Using the following boundary conditions;

$$\delta_b(0) = 0 \tag{12}$$

$$\theta(L/2) = 0 \tag{13}$$

The two coefficients ($\theta_0$ and $\delta_{b0}$) in equations 10 and 11 are calculated and they can be write

$$\theta(x)=\int_0^x \gamma(M(\eta))\, d\eta - \int_0^{L/2} \gamma\,(M(\eta))\, d\eta = \int_{L/2}^x \gamma(M(\eta))d\eta \quad (14)$$

$$\delta_b\,(x)=\int_0^x \theta(\eta)\, d\eta \quad (15)$$

For the maximum beam deflection (at mid-span), the upper bound of Equation (15) is L / 2.

3.2.2. Deflection due to shear force

To determine the shear deflection of beams, the unit load method was used;

$$\delta_s\,(x)=\int_0^x \alpha \frac{\upsilon V}{G A_e} d\eta \quad (16)$$

Where υ and V are shear forces due to the unit load and applied load, respectively.

For rectangular cross section the following coefficient value is used;

$$\alpha = \frac{6}{5} \quad (17)$$

And the effective shear area is as follows:

$$A_e = b\left(\frac{c+h}{2}\right) \quad (18)$$

And shear modulus is provided as:

$$G = \frac{E_t}{2(1+\nu)} \quad (19)$$

Where

$$E_t = \frac{E_i + E_u}{2} \quad (20)$$

Here, $E_t$ is the average tangent modulus and $E_i$ , $E_u$ are the initial and ultimate tangent modulus defined as;

$$E_i = \left(\frac{\partial f_c}{\partial \varepsilon_c}\right)_0 = \frac{2}{\varepsilon_0} f_c^{'} = 1000\, f_c^{'} \quad (21)$$

$$E_u = \left(\frac{\partial f_c}{\partial \varepsilon_c}\right)_{\varepsilon_0} = 0 \quad (22)$$

And the poison ratio for concrete is;

$$\nu = 0.15 \quad (23)$$

Now, the total deflection is sum of the deflection due to bending moment and due to shear force.

$$\delta(x) = \delta_b\,(x) + \delta_s\,(x) \quad (24)$$

## 4. Results and discussion

The experimental moment-curvature curves are shown in Fig.s 6 to 8 for reinforced concrete beams made of rebar. Fig.s 9 to 11 illustrates the experimental moment-curvature diagrams for reinforced concrete beams made of cables (tendons).

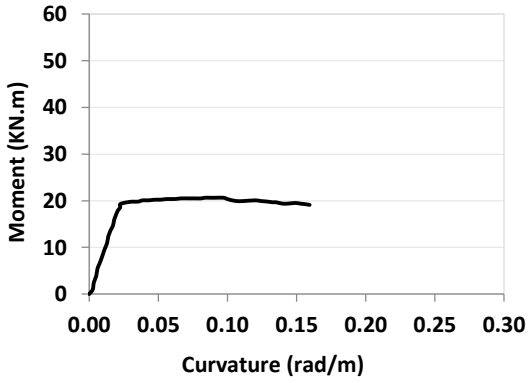


**Fig. 6.** Moment-curvature for rebar beam RB-1.

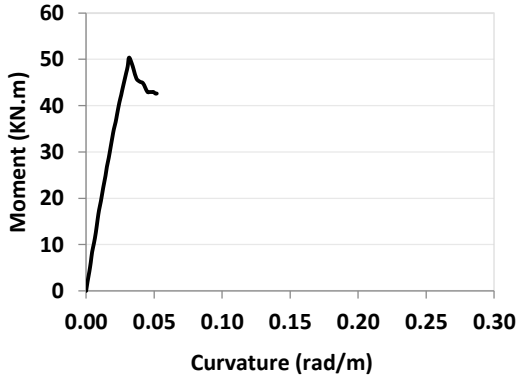


**Fig. 7.** Moment-curvature for rebar beam RB-2.

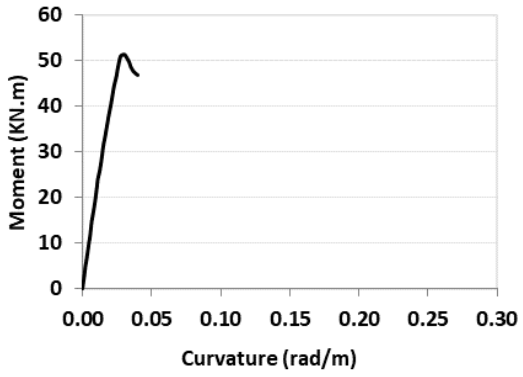


**Fig. 8.** Moment-curvature for rebar beam RB-4.

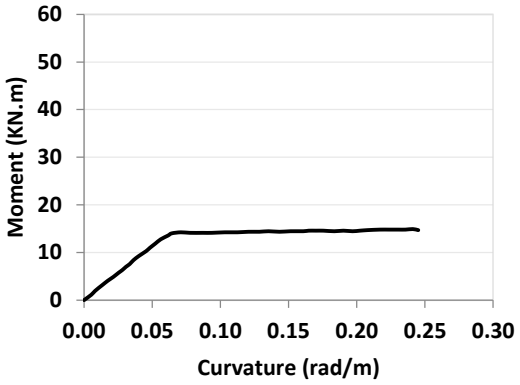


**Fig. 9.** Moment-curvature for cable beam CB-1.

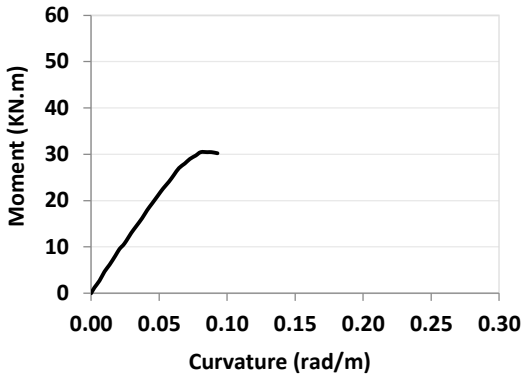


**Fig. 10.** Moment-curvature for cable beam CB-2.

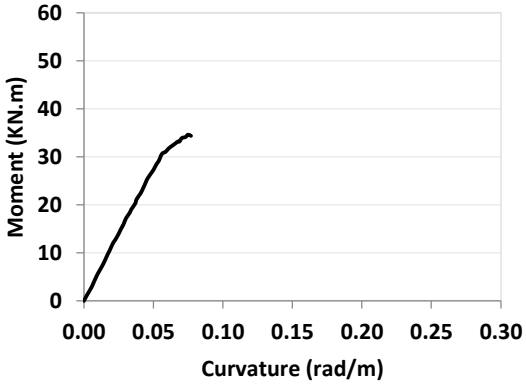


**Fig. 11.** Moment-curvature for cable beam CB-4.

The predicted steel strains when the concrete beams failed are shown in Tables 5 and 6 for beams made with rebar and cable (tendons), respectively. For the under the reinforced beam, steel strain is exceeding the $\varepsilon_y$ (passed the yield point), for the balanced beam $\varepsilon_y$ is equal to $\varepsilon_y$ (just yielded) and for the over reinforced beam, It is less than $\varepsilon_y$ (not yielded yet). This confirms that the ductility principles in regular RC beams can be extended to those reinforced with tendons. It must be mentioned that the yield strength of the steel rebars, as well as the tendons, were obtained from the manufacturer.

**Table 5.** Predicted steel strains as concrete beams with rebar failed.

| | $A_s$ | $F_y$ (MPa) | $\varepsilon_y$ | $\varepsilon_s$ |
|---|---|---|---|---|
| Under-Reinforced | 3ϕ12mm | 400 | 0.00206 | 0.0128 |
| Balanced | 3ϕ22mm | 400 | 0.00206 | 0.00206 |
| Over-Reinforced | 4ϕ22mm | 400 | 0.00206 | 0.00175 |

**Table 6.** Predicted steel strains as concrete beams with tendon failed.

| | $A_s$ | $F_y$ (MPa) | $\varepsilon_y$ | $\varepsilon_s$ |
|---|---|---|---|---|
| Under-Reinforced | 3ϕ6mm | 1550 | 0.0078 | 0.00243 |
| Balanced | 3ϕ10mm | 1674 | 0.0084 | 0.00810 |
| Over-Reinforced | 4ϕ10mm | 1674 | 0.0084 | 0.00697 |

Fig.s 12 to 17 show a comparison of test results versus theoretical values of load-deflection for rebar and cable (tendons) samples. The tests matched with the theoretical results but for heavier reinforced beams, it was not possible to get to the real failure point rather than local concrete crushing at the support points. The load-deflection curves (Fig.s 14, 15, and 18) were following a linear behavior until the beams suddenly broke locally at the support points.

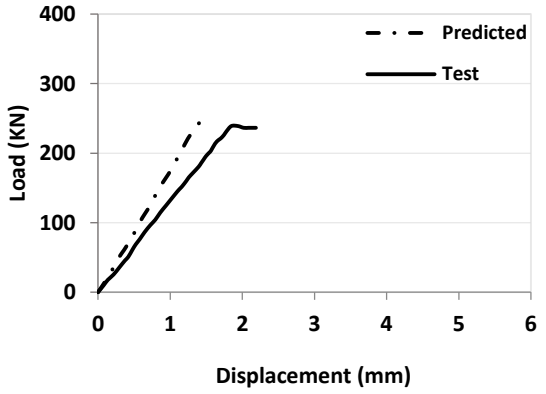


**Fig. 12.** Comparison of test results vs. predicted values of load-deflection for rebar beam RB-1.

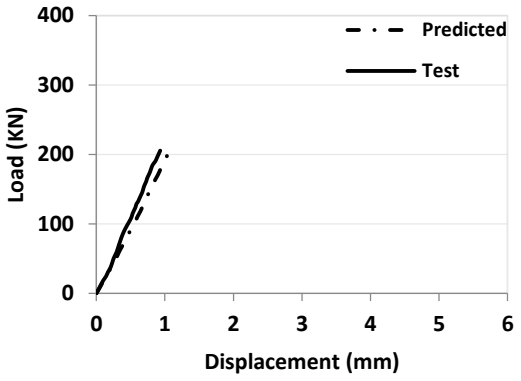


**Fig. 13.** Comparison of test results vs. predicted values of load-deflection for rebar beam RB-3.

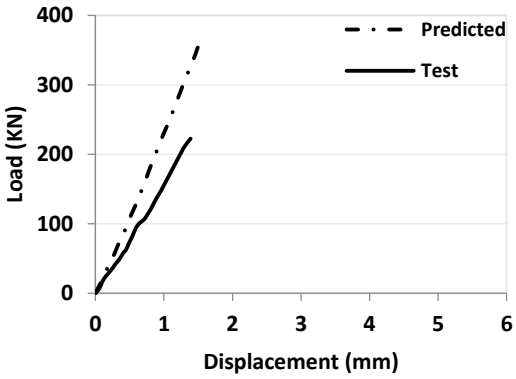


**Fig. 14.** Comparison of test results vs. predicted values of load-deflection for rebar beam RB-4.

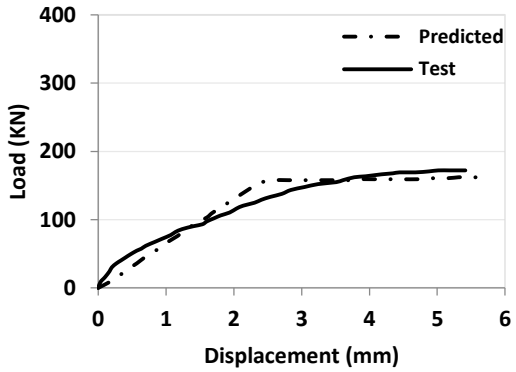


**Fig. 15.** Comparison of test results vs. predicted values of load-deflection for cable beam CB-1.

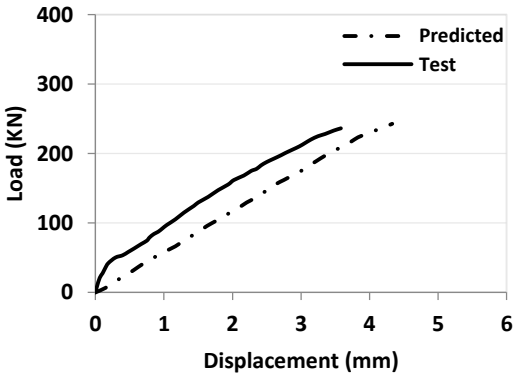


**Fig. 16.** Comparison of test results vs. predicted values of load-deflection for cable beam CB-3.

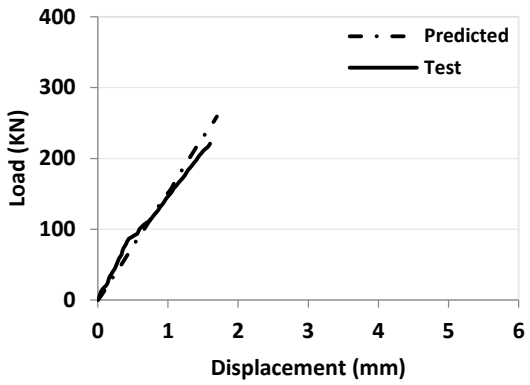


**Fig. 17.** Comparison of test results vs. predicted values of load-deflection for cable beam CB-4.

Now as an example to show how the flexural strength of the reinforcement concrete beams with non-prestressed tendons can be accurately predicted, beam CB 1 is considered. Using the conventional reinforced concrete beams equations, we can calculate the nominal bending moment capacity; as follows:

$$M_n = A_s F_y \left(d - \frac{A_s F_y}{1.7 b f_c'}\right)$$

$$= (3 \times 23.23) \times 1550 \times \left(157 - \frac{(3 \times 23.23) \times 1550}{1.7 \times 180 \times 39.6}\right)$$

$$= 15996 \ \text{(KN.mm)}$$

Thus, the corresponding loads on the beam that would cause this maximum moment in the beam can be obtained; as follows:

$$\frac{P}{2} = \frac{M_n}{(500 - 150)/2}$$

Therefore,

$$P = 183 \quad \text{(KN)}$$

This value matches very well with the picked load in Fig. 15.

## 5. Conclusions

The load-deflection curves were measured and compared with the theoretically predicted values. The theoretical model was able to predict the experimental load-deflection curves almost accurately. Results also showed close predicted stiffness values compared to test results, as well. So, it was demonstrated that the same concepts of the normal reinforced concrete beams can be applied for reinforced concrete beams using tendons as main reinforcement for both stiffness and strength calculations. For beams with heavier steel ratios, more studies are required on beams with a lower aspect ratio (longer beams). This paper is not trying to recommend any type of direct comparison between RC beams using rebar vs. tendons because their stress-strain properties are different but it is trying to show the same principles could be applied, if tendons are used, to predict the behavior of these beams. So, this paper is not trying to come up with an equivalent area of a tendon that would be similar to a given area of rebar but it is presenting the same principles that can be used to design RC beam using tendons, for a given load.

## Credit authorship contribution statement

S.M.R Mortazavi: Project administration, Supervision, Writing-original draft, Validation, Conceptualization, Methodology. Milad Shakiba: Investigation, Resources, Writing-original draft, Writing-review&editing, Formal analysis, Conceptualization, Validation, Methodology.

## Declaration of competing interest

The authors declare that they have no known competing financial interests or personal relationships that could have appeared to influence the work reported in this paper.

## Acknowledgment

The authors would like to thank Shahid Rajaee Teacher Training University staff for their kind support and help. Besides, the research has not received any specific fund or grant.

## Nomenclature

$C_C$ the compressive force of the concrete

$T_S$ the tension force of the reinforcing steel

$A_S$ the cross-sectional area of the tension reinforcing steel

$f_S$ the stress in the tension reinforcing steel

$\varepsilon_C$ the concrete compressive strain at the extreme compression fiber

$\varepsilon_S$ the tensile strain of the reinforcing steel

c the distance from the neutral axis to the extreme compression fiber of the concrete

d the distance from the centroid of the tension reinforcing steel to the extreme compression fiber of the concrete

$\varepsilon_y$ the yield strain of the reinforcing steel

$E_S$ the modulus of elasticity of the tension reinforcing steel

E the modulus of elasticity of the tendon reinforcement

$f_y$ the yield stress of the reinforcing steel

$f'_C$ the maximum compressive stress of concrete

$\varepsilon_C$ concrete strain at any given point

$\varepsilon_O$ the strain at the maximum compressive stress of concrete, and is defined as 0.002

$\gamma$ the beam curvature

y distance measured from the neutral axis

$\alpha$ the mean stress factor, and define as 0.85

b the width of the concrete beam

x distance from the section under consideration to the end support

$\eta$ variable of integration, distances from support for sections between 0 up to section at x

$\theta_0$ beam rotation at the support

$\delta_{b0}$ beam deflection at the support

## REFERENCES

[1] S. A. Mirza and B. W. Skrabek, "Reliability of short composite beam-column strength interaction," *J. Struct. Eng.*, vol. 117, no. 8, pp. 2320–2339, 1991.

[2] S. A. Mirza and B. W. Skrabek, "Statistical analysis of slender composite beam-column strength," *J. Struct. Eng.*, vol. 118, no. 5, pp. 1312–1332, 1992.

[3] J. M. Ricles and S. D. Paboojian, "Seismic performance of steel-encased composite columns," *J. Struct. Eng.*, vol. 120, no. 8, pp. 2474–2494, 1994.

[4] A. Khaloo, H. Moradi, A. Kazemian, and M. Shekarchi, "Experimental investigation on the behavior of RC arches strengthened by GFRP composites," *Constr. Build. Mater.*, vol. 235, p. 117519, 2020.

[5] P. R. Munoz and C.-T. T. Hsu, "Behavior of biaxially loaded concrete-encased composite columns," *J. Struct. Eng.*, vol. 123, no. 9, pp. 1163–1171, 1997.

[6] S. El-Tawil and G. G. Deierlein, "Strength and ductility of concrete encased composite columns," *J. Struct. Eng.*, vol. 125, no. 9, pp. 1009–1019, 1999.

[7] S. A. Mirza and E. A. Lacroix, "Comparative strength analyses of concrete-encased steel composite columns," *J. Struct. Eng.*, vol. 130, no. 12, pp. 1941–1953, 2004.

[8] M. Esfahani, M. Hoseinzade, M. Shakiba, F. Arbab, M. Yekrangnia, and G. Pachideh, "Experimental investigation of residual flexural capacity of damaged reinforced concrete beams exposed to elevated temperatures," *Eng. Struct.*, vol. 240, p. 112388, 2021.

[9] A. A. Abdelrahman, N. M. Nofel, A. H. Ghallab, T. H. El-Afandy, and A. Mahmoud, "Behavior of prestressed concrete beams subjected to fire," *Hous. Build. Natl. Res. Cent. J.*, vol. 7, pp. 38–55, 2011.

[10] W. Yuan, G. Gan, and W. Jin, "Study on prestressed steel reinforced concrete structures subjected to bending moment," *J. Harbin Inst. Technol.*, vol. 35, no. 1, pp. 116–119, 2003.

[11] X. Xiong, G. Yao, and X. Su, "Experimental and numerical studies on seismic behavior of bonded and unbonded prestressed steel reinforced concrete frame beam," *Eng. Struct.*, vol. 167, pp. 567–581, 2018.

[12] V. Borzovič, J. Laco, M. Pecník, and P. Pažma, "The Crack Development Mechanism of Prestressed Girder Influenced by Different Bond between Prestressed Tendons and Concrete," in *Key Engineering Materials*, 2016, vol. 691, pp. 309–320.

[13] X. Tao and G. Du, "Ultimate stress of unbonded tendons in partially prestressed concrete beams," *PCI J.*, vol. 30, no. 6, pp. 72–91, 1985.

[14] T. I. Campbell and K. L. Chouinard, "Influence of Nonprestressed Reinforcement on Strength of Unbonded Partially prestressed concrete members," *Struct. J.*, vol. 88, no. 5, pp. 546–551, 1991.

[15] W. An, H. Saadatmanesh, and M. R. Ehsani, "RC beams strengthened with FRP plates. II: Analysis and parametric study," *J. Struct. Eng.*, vol. 117, no. 11, pp. 3434–3455, 1991.

[16] H. Saadatmanesh and M. R. Ehsani, "RC beams strengthened with GFRP plates. I: Experimental study," *J. Struct. Eng.*, vol. 117, no. 11, pp. 3417–3433, 1991.

[17] F. T. K. Au and J. S. Du, "Partially prestressed concrete," *Prog. Struct. Eng. Mater.*, vol. 6, no. 2, pp. 127–135, 2004.

[18] H.-G. Kwak and J. H. Kim, "Numerical models for prestressing tendons in containment structures," *Nucl. Eng. Des.*, vol. 236, no. 10, pp. 1061–1080, 2006.

[19] A. H. Ghallab, "Deflection of Externally Prestressed Continuous RC Beams."

[20] I. F. Kara, A. F. Ashour, and M. A. Köroğlu, "Flexural performance of reinforced concrete beams strengthened with prestressed near-surface-mounted FRP reinforcements," *Compos. Part B Eng.*, vol. 91, pp. 371–383, 2016.

[21] T. C. Triantafillou and N. Plevris, "Strengthening of RC beams with epoxy-bonded fibre-composite materials," *Mater. Struct.*, vol. 25, no. 4, pp. 201–211, 1992.

[22] A. Ghallab and A. W. Beeby, "Ultimate strength of externally strengthened prestressed beams," *Proc. Inst. Civ. Eng. Build.*, vol. 152, no. 4, pp. 395–406, 2002.

[23] H. A. Rasheed, H. Charkas, and H. Melhem, "Simplified nonlinear analysis of strengthened concrete beams based on a rigorous approach," *J. Struct. Eng.*, vol. 130, no. 7, pp. 1087–1096, 2004.

[24] A. Ghallab, "Assessment of Egyptian code for prestressing tendons stress at ultimate flexure," *Sci Bull Fac Eng, Ain Shams Univ*, vol. 41, no. 1, pp. 63–83, 2006.

[25] A. Ghallab, "Calculating ultimate tendon stress in externally prestressed continuous

concrete beams using simplified formulas," *Eng. Struct.*, vol. 46, pp. 417–430, 2013.

[26] M. Hamrat *et al.*, "Experimental and numerical investigation on the deflection behavior of pre-cracked and repaired reinforced concrete beams with fiber-reinforced polymer," *Constr. Build. Mater.*, vol. 249, p. 118745, 2020.

[27] S. A. Bhutta, "Analytical modeling of hybrid composite beams." Virginia Tech, 1993.

[28] N. Zhang, C. C. Fu, and H. Che, "Experiment and numerical modeling of prestressed concrete curved slab with spatial unbonded tendons," *Eng. Struct.*, vol. 33, no. 3, pp. 747–756, 2011.

[29] M. Shakiba, A. V. Oskouei, M. Karamloo, and A. Doostmohamadi, "Effect of mat anchorage on flexural bonding strength between concrete and sand coated GFRP bars," *Compos. Struct.*, vol. 273, p. 114339, 2021.

[30] F. M. Alkhairi and A. E. Naaman, "Analysis of beams prestressed with unbonded internal or external tendons," *J. Struct. Eng.*, vol. 119, no. 9, pp. 2680–2700, 1993.

[31] A. Ghallab and A. W. Beeby, "Calculating stress of external prestressing tendons," *Proc. Inst. Civ. Eng. Build.*, vol. 157, no. 4, pp. 263–278, 2004.

[32] J. Y. Zeng and X. Z. Su, "Internal force system and current secondary moment concept in prestressed structures," in *Applied Mechanics and Materials*, 2014, vol. 501, pp. 611–619.

[33] S. C. M. Ho *et al.*, "Inference of bond slip in prestressed tendons in concrete bridge girders," *Struct. Control Heal. Monit.*, vol. 22, no. 2, pp. 289–300, 2015.

[34] C. A. Jones, R. Dameron, and M. Sircar, "Improving the state of the art in FEM analysis of PCCVs with bonded and unbonded prestress tendons," *Nucl. Eng. Des.*, vol. 295, pp. 782–788, 2015.

[35] S. Yuyama, K. Yokoyama, K. Niitani, M. Ohtsu, and T. Uomoto, "Detection and evaluation of failures in high-strength tendon of prestressed concrete bridges by acoustic emission," *Constr. Build. Mater.*, vol. 21, no. 3, pp. 491–500, 2007.

[36] A. C. I. C. 318, "Building Code Requirements for Structural Concrete (ACI 318-19): An ACI Standard; Commentary on Building Code Requirements for Structural Concrete (ACI 318R-19)," 2020.

[37] A. C. I. Committee, "308R-16: Guide to External Curing of Concrete." 2016.

[38] A. C150, "ASTM C150 standard specification for Portland cement," *ASTM Standard Book*. ASTM International West Conshohocken, Pennsylvania, 2016.

[39] A. C. I. Committee, "ACI 211.1-91 Standard Practice for Selecting Proportions for Normal, Heavyweight, and Mass Concrete, no. 9," *Unites States*, pp. 120–121, 2002.

[40] R. Park and T. Paulay, "Reinforced Concrete Structures, John Wiley & Sons," *NY, USA*, 1975.

[41] H. Abbaszadeh, A. Ahani, and M. R. Emami Azadi, "Debonding and Fracture Behavior of Concrete Specimens Retrofitted by FRP Composite," *Comput. Eng. Phys. Model.*, vol. 1, no. 2, pp. 27–40, 1999.